

Numerical Analysis of Soft Soil Reinforced with Geogrid Encased Stone Column



B. K. Pandey, S. Rajesh, and S. Chandra

Abstract The use of geosynthetic encased stone columns for improving very soft soil has been widely recognized both regarding economy and performance. The stone columns are encased to offer lateral confinement against bulging which causes excessive settlement. In this study, the analysis of the embankment, resting on very soft soil reinforced with stone column encased from geogrid is carried out to understand its behavior. In this study a comprehensive numerical analysis is executed to study the consequence of encasement parameters like its length and stiffness on the on time-dependent behavior of the system. The result of the study shows significant improvement regarding settlement reduction and lesser lateral bulging of the column. Moreover, it also shows that encasing the column fully perform better as compared to the partially encased column. Similarly, using stiffness of geogrid beyond 5000 kN/m does not show substantial improvement.

Keywords Stone column · Soil improvement · Geogrid

1 Introduction

The use of stone columns has proven efficacious both regarding economy and performance. Moreover, it is very successful because of its advantages. It helps in slope stability improvement, increasing bearing capacity and the time rate of settlement, reduction in both differential and total settlement, reducing liquefaction potential [1, 2]. The application of a stone column serves its purpose if the undrained shear strength (C_u) of soil lies between 15 and 50 kPa. However, if the undrained shear strength of the soil is < 15 kPa, then the confinement provided to the stone column by the surrounding soil is inadequate, and hence it fails in excessive settlement due to bulging. Therefore, reinforcing the stone column either by encasement or by placing the horizontal strip of geosynthetic along the length of the column, these two approaches provides the extra resistance against radial bulging of the column as

B. K. Pandey (✉) · S. Rajesh · S. Chandra
Department of Civil Engineering, IIT Kanpur, Kanpur, Uttar Pradesh 208016, India
e-mail: balbir@iitk.ac.in

© Springer Nature Singapore Pte Ltd. 2022
A. K. Dey et al. (eds.), *Proceedings of the 7th Indian Young Geotechnical Engineers Conference*, Lecture Notes in Civil Engineering 195,
https://doi.org/10.1007/978-981-16-6456-4_8

stated by Alexiew et al. [3] and Ali et al. [4]. In last two decades various projects for the railroad and road embankment, bridge ramp, flood protection dike were accomplished using encased stone columns in Germany, Netherland, Sweden, and India [5, 6].

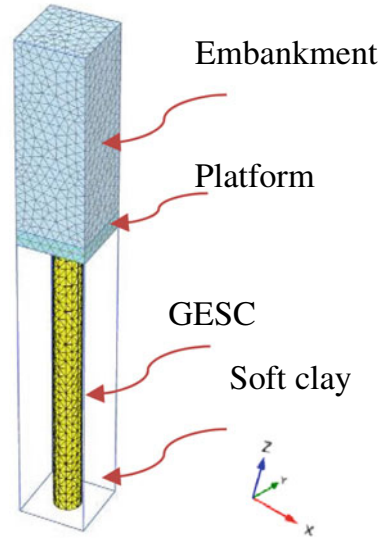
The idea of encasing the column in full or part is studied experimentally by numerous researchers like Rathiel et al. [6] and Murugesan and Rajagopal [7] under undrained condition. In discovering the performance of geogrid encased stone columns (GESCs), numerical modeling has also been extensively used. Yoo and Kim [8] adopted a unit cell (both 3D and axisymmetric) and full 3D model to compare the different modeling approach. Yoo [9] reported the effects of various parameters by modeling quarter of column and full 3D model. Majority of the studies focus on unit cell approach (either 3D or axisymmetric or quarter column) by loading the column only or entire unit cell ([10, 11] and others) or unit cell with embankment loading [12–15]. However, an only limited study has been conducted in details considering the encasement parameter's (length and stiffness) on time-dependent responses under embankment loading. Therefore, there is a need for a comprehensive study to understand the modeling details as well as the behavior of GESC under the embankment loading.

This study focuses on understanding the consequence of encasement length, encasement on the performance of geogrid encased stone column under embankment loading through 3D unit cell model. The impact of the parameters mentioned above is evaluated regarding settlement reduction and lateral deformation of the column along its length.

2 Geometry and Model Description

A finite element package Plaxis 3D [16] is used in the numerical analysis, where a hypothetical case study is formulated. The soil layer consists of 9.5 m of soft clay underlying a 0.5 m of the sand platform. The sand platform is laid before the construction of the embankment, and it serves as the drainage blanket. The ground water table lies at 0.5 m below the ground. The dimension of the unit is 2 m \times 2 m \times 10 m (L \times B \times H) with column installed at the center of the unit cell. The dimension of the unit cell is chosen based on a square pattern of installation having a spacing of 2 m between the columns. The diameter (d) of column adopted in the study is 0.8 m which is equivalent to the area replacement ratio of 12.5% as reported in Balbir et al. (2018). Figure 1 displays the details of the mesh connectivity plot of GESC reinforced soft ground. In the present study, the length of GESC (L_{GESC}) is varied between 5 and 10 m, and the axial stiffness of encasement is varied between 500 and 6000 kN/m [7, 17]. The embankment is constructed in three stages; having a height of 2 m in each stage similar to Yoo [9]. The duration of each stage consists of two parts. First part is a construction period of 20 days succeeded by a 30 days of rest period.

Fig. 1 Generated mesh connectivity plot and details for 3D unit cell



The hydraulic and deformation boundary conditions for the model are chosen based on the symmetry. Therefore, considering symmetry into account no displacement in the perpendicular direction of the symmetry plane and to the base is allowed [9]. Congruently, at the symmetry plane, no flow at the boundary will take place. Therefore, the symmetry plane has been kept as a closed consolidation boundary. Moreover, the bottom boundary is also held closed consolidation boundary considering the impervious layer below the soft clay [10]. The soft soil constitutive material model has been used for modeling the soft soil. However, for the embankment, stone column, and sand platform the Mohr–Coulomb material model is used. Table 1 summarizes the constitutive model and related parameters used in the analysis. The geogrid is used in the study and is modeled as an elastic material having orthotropic behavior. The soft soil, sand platform, and embankment were modeled using twelve node tetrahedral elements. The geogrid was modeled using six node triangular surface element. For modeling soil-geogrid interaction, joint elements (interfaces) were added to geogrid and surrounding soil. The interfaces comprise of twelve node interface elements with zero thickness. The R_{inter} adopted in the present study for soft soil, sand platform, embankment, and stone column are one as reported by Aljanabi et al. [18], whereas for geogrid soil interface it is 0.7 as reported by Chen et al. [19] and Pandey et al. [20]. These are slender structures that can sustain only tensile force and no compression. The present study is validated with the study conducted by Rajesh [10] in which the surface load is applied to the top of an axisymmetric problem.

However, in the present study, 3D unit cell having a square cross-sectional area of dimension 2.25×2.25 m is used as reported by Rajesh [10]. All the material properties and the dimensions were kept intact, except properties of the plate. A steel plate of thickness (t_p) 30 mm, unit weight of steel (γ_{steel}) = 78.5 kN/m³ and E =

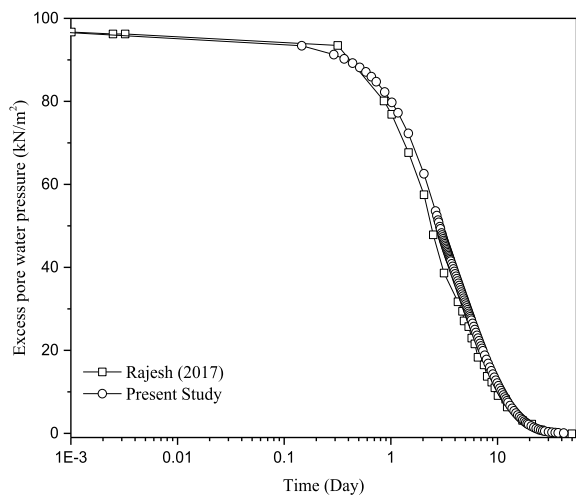
Table 1 Summary of the constitutive model and related parameter

	Column (Mohr–Coulomb)	Soft clay (soft soil)	Platform (Mohr–Coulomb)	Embankment (Mohr–Coulomb)
Properties	Chen et al. [19]	Hosseinpour et al. [14]	Huang et al. [21]	Aljanabi et al. [18]
γ (kN/m ²)	22	14.50	20	20
E (kPa)	40,000	750	20,000	20,000
ν	0.30	0.28	0.33	0.30
c' (kPa)	0.50	4	5	5
φ' (0°)	38	27.50	32	30
Ψ (0°)	10	–	–	–
C_c	–	1.26	–	–
C_s	–	0.097	–	–
kh (m/day)	10.368	7.50×10^{-5}	1	1
k _v (m/day)	10.368	8.40×10^{-5}	1	1

Note E = Tangential elastic modulus; ν = Poisson’s ratio; γ = Soil unit weight; c' = Cohesion of Soil; φ' = Soil friction angle; ψ = Dilation angle; C_c = Compressibility index; C_s = Swelling Index; k = Permeability (Subscript h and ν corresponds to Horizontal and vertical respectively); – = Data not given

4.44×10^6 kN/m² is used for the loading. The linear isotropic constitutive model has been adopted for steel plate. The details of the constitutive model and related parameters for other materials can be found in the referred paper. Figure 2 shows the result of the 3D unit cell compared with the axisymmetric model of Rajesh [10] for soft soil reinforced with ordinary stone column (OSC). The results show that the model is in good agreement with the referred study.

Fig. 2 Validation with Rajesh [10] for OSC (very fine mesh)



3 Outcomes and Discussion

The primary emphasis in the present paper is to understand the consequence of encasement parameters like its stiffness and length on the performance of the geogrid reinforced stone column.

3.1 Effect of Length of Encasement

The impact of length of encasement on the behavior of GESG is analyzed by varying encasement length (ζ) between zero and one. The reference encasement stiffness used for this parametric study is 2000 kN/m. In Fig. 3, settlement reduction factor (β) is plotted against embankment resting on GESG improved ground having varying encasement length. From this figure, it can be observed that column encased fully results in a significant diminution in the settlement ($> 61\%$) as compared to the column without encasement. Moreover, the variance in the settlement reduction (β) for $\zeta = 0.75$ and $\zeta = 0.85$ w.r.t, $\zeta = 1$ is approximately 21% and 16%, respectively. Seeing this variation, one can state that the column encased fully contributes a significant decrease in the settlement when compared to partially encase. Additionally, the column bulging laterally is dominant at the location where encasement terminates at the bottom as can be noticed from Fig. 4. In this figure, lateral deformation is plotted against column depth of GESG for various length of encasement as stated above. However, the deformation in the case of the column encased fully is almost twice as equated to the column without encasement (i.e., OSC) at the point of termination of the encasement (example let us say at 5 m from the top for $\zeta = 0.50$).

Fig. 3 Settlement reduction factor for embankment resting on GESG having varying length of GESG

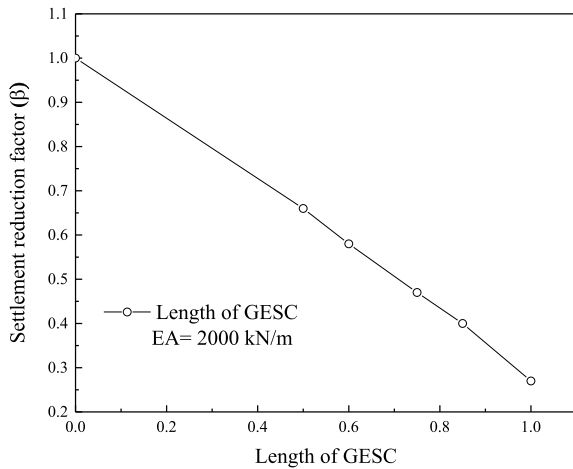
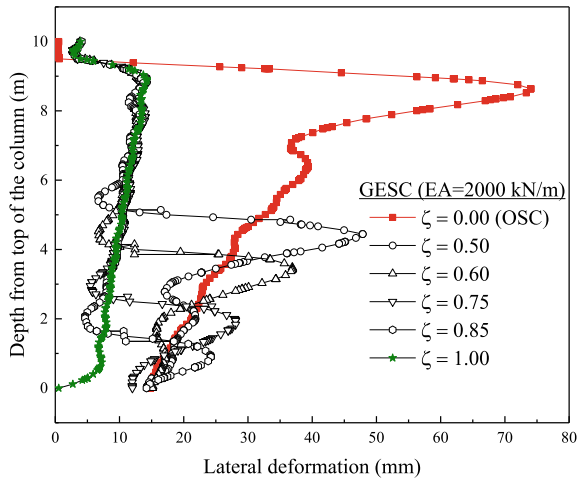


Fig. 4 Lateral deformation of GESC having different encasement length



3.2 Effect of Encasement Stiffness

To weigh the impact of geogrid stiffness, its axial stiffness is varied between 500 and 6000 kN/m. In Fig. 5, settlement reduction factor (β) is plotted against GESC improved ground having different encasement stiffness. However, from this figure we can, clearly, see that the difference in the settlement reduction by using GESC with encasement having stiffness 6000 kN/m is inconsequential (approx. 8%) as compared to encasement having 5000 kN/m stiffness. Therefore, we can state that using encasement stiffness above 5000 kN/m has no determinantal effect.

Figure 6 illustrates the lateral deformation of the OSC and GESC having the different stiffness of the encasement. As expected the lateral deformation in the case of OSC is 14.43 times higher as compared to GESC with the stiffness of 6000 kN/m.

Fig. 5 Settlement reduction factor for GESC improved ground having different encasement stiffness

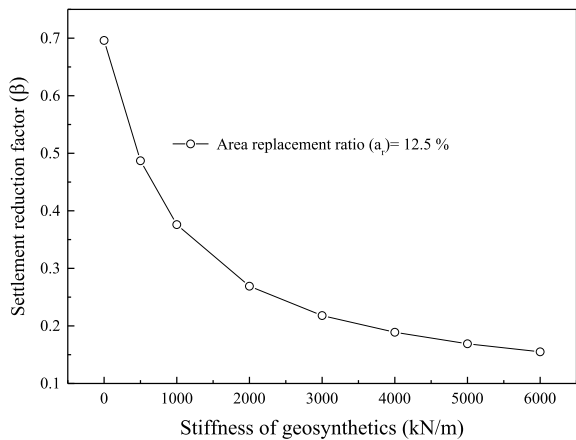
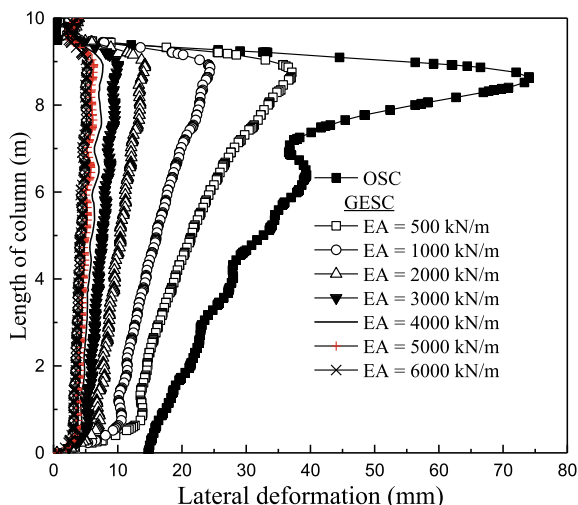


Fig. 6 Lateral deformation of the column of OSC and GESC for different encasement stiffness



However, it is 1.18 times for the encasement stiffness 5000 kN/m as compared to 6000 kN/m. From the previous studies [2, 8] the maximum lateral deformation occurs at the depth varying between 2 and 3*D from the top of the column. This maximum deformation depth is dependent on the loading area as well as the strength of the surrounding soil. In the current study as can be seen from Fig. 6, this depth is nearly 1.7*D.

4 Conclusion

The paper presents an organized numerical analysis of embankment resting on a stone column encased with geogrid. The area replacement ratio study is kept constant at 12.5% during the analysis. From the study, the following points are concluded.

1. The fully encased stone column shows better performance as compared to a partially encased column regarding both settlement reduction and in prevention of radial bulging of the column.
2. It is observed that when the column is partially encased, maximum bulging occurs at the location where encasement terminates.

References

1. Abhishek SV, Rajyalakshmi K, Madhav MR (2016) Int J Geotech Eng 10(4):337–357
2. Barksdale RD, Bachus RC (1983) Design and construction of stone column, vol 1. U.S Department of Transportation, Report No-FHA FHWA/RD-83

3. Alexiew D, Raithel M, Kuster V, Detert O (2012) 15 years of experience with geotextile encased granular columns as foundation system. In: ISSMGE-TC 211 International symposium on ground improvement. IS-GI, Brussels
4. Ali K, Shahu JT, Sharma KG (2012) Model tests on geosynthetic-reinforced stone columns: a comparative study. *Geosynth Int* 19(4):292–305
5. Mahajan R, Korulla M, Rimoldi P (2016) Geotextile encased columns design and installation. In: Proceedings of the 6th Asian regional conference on geosynthetics—geosynthetics for infrastructure development. New Delhi, India:188–194 (2016).
6. Raithel M, Kirchner A, Schade C, Leusink E (2005) Foundation of construction on very soft soil with geotextile encased column-state of the art. In: Proceedings of Geo-frontiers 2005. Austin, Texas, United States, pp 1–11
7. Murugesan S, Rajagopal K (2006) Geosynthetic-encased stone columns: Numerical evaluation. *Geotext Geomembr* 24:349–358
8. Yoo C, Kim S-B (2009) Numerical modeling of geosynthetic-encased stone column-reinforced ground. *Geosynthetic Int* 16:116–126
9. Yoo C (2010) Performance of geosynthetic-encased stone columns in embankment construction: numerical investigation. *J Geotech Geoenviron Eng* 136:1148–1160
10. Rajesh S (2017) Time-dependent behaviour of fully and partially penetrated geosynthetic encased stone columns. *Geosynthetic Int* 24:60–71
11. Rajesh S, Jain P (2015) Influence of permeability of soft clay on the efficiency of stone columns and geosynthetic encased stone columns—a numerical study. *Int J Geotech Eng* 9(5):483–493
12. Almeida MSS, Riccio M, Hosseinpour I (2013) Performance of a geosynthetic-encased column (GEC) in soft ground: numerical and analytical studies. *Geosynthetic Int* 20:252–262
13. Elsayw MBD (2013) Behavior of soft ground improved by conventional and geogrid-encased stone columns, based on FEM study. *Geosynthetic Int* 20:276–285
14. Hosseinpour I, Riccio M, Almeida MSS (2014) Numerical evaluation of a granular column reinforced by geosynthetics using encasement and laminated disks. *Geotext Geomembr* 42:363–373
15. Zhang L, Zhao M (2015) Deformation analysis of geotextile-encased stone columns. *Int J Geomech* 15:1–10
16. Brinkgreve RBJ, Engin E, Swolf WM (2013) *Plaxis 3D 2013 Manual*. Plaxis Bv. The Netherland
17. Khabbazian M, Kaliakin VN, Meehan CL (2010) Numerical study of the effect of geosynthetic encasement on the behaviour of granular columns. *Geosynthetic Int* 17:132–143
18. Aljanabi QA, Chik Z, Kasa A (2013) Construction of a new highway embankment on the soft clay soil treatment by stone columns in Malaysia. *J Eng Sci Technol* 8:448–456
19. Chen J-F, Li LY, Xue J-F, Feng S-Z (2015) Failure mechanism of geosynthetic-encased stone columns in soft soils under embankment. *Geotext Geomembr* 43:424–431
20. Pandey BK, Rajesh S, Chandra S (2018) 3-D finite element study of embankment resisting on soft soil reinforced with encased stone column. In: Proceedings of Indian geotechnical conference. Bangalore, pp 1–8
21. Huang J, Han J, Oztoprak S (2009) Coupled mechanical and hydraulic modeling of geosynthetic-reinforced column-supported embankments. *J Geotech Geoenviron Eng* 135(8):1011–1021